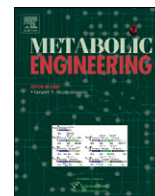




ELSEVIER

Contents lists available at ScienceDirect

Metabolic Engineering

journal homepage: www.elsevier.com/locate/ymben

Catching prompt metabolite dynamics in *Escherichia coli* with the BioScope at oxygen rich conditions

Marjan De Mey^{a,b,1}, Hilal Taymaz-Nikerel^{b,1}, Gino Baart^c, Hendrik Waegeman^a, Jo Maertens^c, Joseph J. Heijnen^b, Walter M. van Gulik^{b,*}

^a Department of Biochemical and Microbial Technology, Ghent University, Coupure Links 653, 9000 Ghent, Belgium

^b Department of Biotechnology, Delft University of Technology, Kluuyver Centre for Genomics of Industrial Fermentation, Julianalaan 67, 2628 BC Delft, The Netherlands

^c Department of Applied Mathematics, Biometrics and Process Control, Ghent University, Coupure Links 653, 9000 Ghent, Belgium

ARTICLE INFO

Article history:

Received 1 March 2010

Received in revised form

12 April 2010

Accepted 26 April 2010

Available online 4 May 2010

Keywords:

Escherichia coli

BioScope

Stimulus response experiments

Glucose pulse

In vivo kinetics

ABSTRACT

The design and application of a BioScope, a mini plug-flow reactor for carrying out pulse response experiments, specifically designed for *Escherichia coli* is presented. Main differences with the previous design are an increased volume-specific membrane surface for oxygen transfer and significantly decreased sampling intervals. The characteristics of the new device (pressure drop, residence time distribution, plug-flow behavior and O₂ mass transfer) were determined and evaluated. Subsequently, 2.8 mM glucose perturbation experiments on glucose-limited aerobic *E. coli* chemostat cultures were carried out directly in the chemostat as well as in the BioScope (for two time frames: 8 and 40 s). It was ensured that fully aerobic conditions were maintained during the perturbation experiments. To avoid metabolite leakage during quenching, metabolite quantification (glycolytic and TCA-cycle intermediates and nucleotides) was carried out with a differential method, whereby the amounts measured in the filtrate were subtracted from the amounts measured in total broth. The dynamic metabolite profiles obtained from the BioScope perturbations were very comparable with the profiles obtained from the chemostat perturbation. This agreement demonstrates that the BioScope is a promising device for studying *in vivo* kinetics in *E. coli* that shows much faster response (< 10 s) in comparison with eukaryotes.

© 2010 Elsevier Inc. All rights reserved.

1. Introduction

Metabolic engineering, the modification of specific biochemical reactions of an organism and/or the introduction of new ones with the use of recombinant DNA-technology, can be applied for the directed improvement of product formation in industrial microorganisms (Stephanopoulos, 1999). Hereby it should be realized that the product pathway to be engineered is always part of a larger metabolic network, designed to serve the benefit of the organism and controlled by the latter through a hierarchy of regulatory interactions. Generally the product pathway withdraws carbon precursors, metabolic energy (ATP) and reducing equivalents, in the form of NADPH, from central metabolism and produces NADH. The main factors which determine the flux through the product pathway are: (1) the enzyme levels in the pathway, (2) the concentrations of cofactors (ATP, NADPH, NADH)

and (3) the concentrations of the relevant intermediates of central metabolism.

To fully and quantitatively understand the relation between a product pathway and connected central metabolism, mathematical models are indispensable (Krömer et al., 2006; Wiechert, 2002). To allow the quantitative evaluation of the effect of genetic interventions (changing enzyme levels and/or their kinetic properties) on cellular behavior and productivity, dynamic models, based on the kinetic properties of the individual enzymes, are required (Chou and Voit, 2009; Nikerel et al., 2009).

It is common practice to determine enzyme kinetic properties from *in vitro* experiments with isolated enzymes, thereby using optimal conditions for each individual enzyme. However, these conditions rarely resemble the natural environment of enzymes inside the living cell. It has been shown that applying enzyme kinetic properties obtained under *in vitro* conditions for kinetic modeling of the *in vivo* behavior of yeast might lead to erroneous predictions (Teusink et al., 2000). Therefore, there is an urgent need for accurate enzyme kinetic data which are valid under *in vivo* conditions. These can be obtained from perturbations of well defined steady-state conditions of whole cells and requires to measure enzyme levels, fluxes and metabolite levels.

* Corresponding author. Fax: +31 15 2782355.

E-mail address: w.m.vangulik@tudelft.nl (W.M. van Gulik).

¹ Both authors equally contributed to this work.

If perturbation experiments are carried out in a sufficiently short time frame (seconds to several minutes), the enzyme levels can be assumed not to change and hence only intra- and extracellular metabolite concentrations as a function of time are required to obtain the rates from the mass balances.

The rapid perturbation technique was pioneered by Theobald et al. (1993) with the aim to elucidate the *in vivo* kinetic properties of yeast glycolysis. They developed a rapid sampling technique which allowed taking samples from a bench scale bioreactor each 4–5 s. Schaefer et al. (1999) further improved sampling from a stirred tank bioreactor, using an automated rapid sampling device capable of sampling in time intervals of 0.22 s. Hoque et al. (2005) also developed a rapid sampling device enabling to take samples from the reactor within a second. However, a drawback of these approaches is the disturbance of the steady-state condition when carrying out a perturbation experiment. Therefore, only one perturbation experiment can be performed per chemostat. Additionally, the number of different kinds of samples that can be taken is limited, e.g. the samples required for metabolome analysis in the broth and in the supernatant, for transcriptome analysis, for enzyme activity measurements and proteome measurements might be treated differently, which would require repetition of the perturbation and thus multiple steady-state chemostat cultures.

To avoid these disadvantages, Visser et al. (2002) and Buziol et al. (2002) proposed sampling and perturbation devices, which allow performing the perturbations outside the reactor (instead of perturbing the whole culture), based on a stopped-flow technique that was originally used in the work of de Koning and van Dam (1992). The disadvantage of the sampling device of Buziol et al. (2002) is that the maximum time window of sampling is about 20 s for aerobic perturbations because their system does not allow continuous supply of oxygen in the sampling/perturbation device.

An improved stopped-flow technique, allowing oxygenation and thus longer perturbation times, was prototyped by Visser et al. (2002), who introduced the acronym “BioScope” for the device. The system was further improved by Mashego et al. (2006). The BioScope is a mini plug-flow reactor coupled to a

steady-state chemostat and has a gas and a broth channel separated by a silicone membrane for oxygen and carbon dioxide exchange. It is important to emphasize that with the BioScope the amount of sample obtained is, in principle, unlimited and different sampling/quenching protocols can be applied in the same perturbation experiment (e.g. for the measurement of metabolites in total broth and supernatant).

The BioScope device has been successfully used for perturbation experiments in yeast (Kresnowati et al., 2008; Mashego et al., 2007) and filamentous fungi (Nasution et al., 2006). Although the performance of the BioScope in its present configuration has been successful, much shorter sampling time intervals are required for *Escherichia coli* perturbation experiments due to the expected faster reaction dynamics of the *E. coli* central metabolism (Buchholz et al., 2002; Chassagnole et al., 2002; Hoque et al., 2005; Schaefer et al., 1999).

This contribution describes the characterization of a BioScope II device, redesigned for *E. coli* perturbation experiments on a time scale of seconds. The performance of the new device is demonstrated by comparing the results of glucose perturbations carried out in the redesigned BioScope, coupled to a steady-state chemostat culture of *E. coli* with results of similar perturbations carried out directly in the chemostat. Precautions were taken that no oxygen depletion could occur during these perturbation experiments. For metabolite quantification, a differential method was used (Taymaz-Nikerel et al., 2009) whereby the intracellular metabolite levels were obtained from measurements in total broth and filtrate samples.

2. Materials and methods

2.1. BioScope design

The design of the BioScope (Fig. 1) adapted for *E. coli* perturbation experiments was based on the 2nd generation BioScope (BioScope II) developed for perturbation experiments in yeast (Mashego et al., 2006). Modification of BioScope II to fulfil

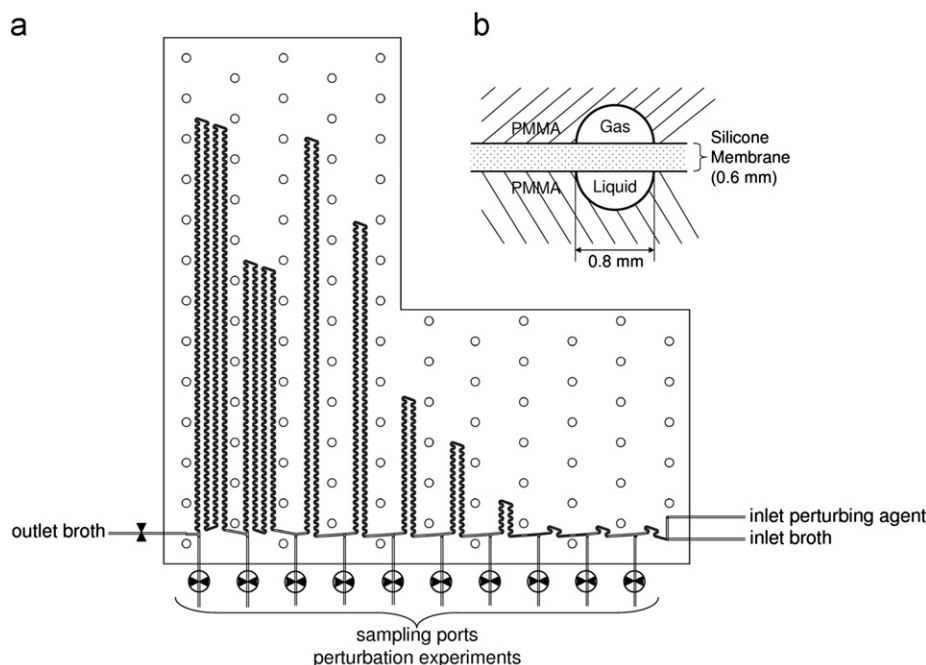


Fig. 1. (a) 2D serpentine channel geometry of the BioScope and (b) cross-section of the BioScope channel.

the requirements for *E. coli* perturbation experiments was aimed at meeting relevant criteria as

- Sufficient oxygen transfer capacity and plug-flow characteristics.
- A high sampling frequency, with a time interval of maximally 1 s between samples, is required for the first 4 subsequent sampling ports to catch the expected fast initial reaction dynamics of *E. coli* (Buchholz et al., 2002; Chassagnole et al., 2002; Hoque et al., 2005; Schaefer et al., 1999).
- No disturbance of the steady-state conditions of the chemostat. Therefore the inflow rate of the BioScope should not exceed the outflow rate of the chemostat culture.
- The pressure drop over the total channel should be less than 1 bar to prevent possible damage to the channel. Additionally, the cassette used in the pump-head is not recommended to be operated at differential pressures above 1 bar (ISMATEC, Glattbrugg, Switzerland).

To decrease the residence time in the BioScope without significantly increasing the through flow rate, the working volume was decreased. This was accomplished by reducing the internal diameter of the BioScope II channel from 1.2 to 0.8 mm and the channel length from 6.51 to 4.00 m. This resulted in a decrease of the volume of the BioScope from the original 3.5 to 1.005 ml.

A LabVIEW (National Instruments Corporation, Austin, TX, USA) script was used to control a series of magnetic pinch valves for withdrawal of samples at different channel positions. The sampling ports were situated at the following channel volumes relative to the substrate addition point: 0.010, 0.022, 0.034, 0.056, 0.101, 0.165, 0.297, 0.461, 0.678 and 1.005 ml corresponding to sampling ports 1–10, respectively, as indicated in Fig. 1. The corresponding residence times for the different sampling ports depends on the applied through flow rate, whereby increasing the through flow rate leads to decreased residence times and vice versa. This design would shorten the maximal observation time window for 10 samples, e.g. to 30.2 s at 2 ml/min, and hence if it is desired to have a shorter observation window, a faster flow rate should be used.

2.2. Pressure drop, residence time distribution (RTD) and oxygen transfer

Oxygenation of and CO₂ removal from the broth in the BioScope channel was achieved via the silicone membrane separating the liquid and the gas channels. The pressure drop over the liquid channel was measured at each sample port for different broth flow rates.

The residence time distribution for the different sample ports was measured by a tracer response experiment as described previously (Mashego et al., 2006; Visser et al., 2002). First, the BioScope channel was flushed with deionized water, then at $t=0$ the water flow was changed to a 1.0N KCl solution and the response at every port was measured with a conductivity meter (Dionex, Sunnyvale, USA). RTD measurements were carried out for flow rates of 2 and 4 ml/min in fivefold. The RTD of the flow cell was measured separately, using the same method. All data were monitored using an in-house made program in LabVIEW (National Instruments Corporation, Austin, TX, USA). Afterwards the raw time and conductivity data were used as an input for a home-made computer program that calculates the mean residence time of every port and its variance by first computing the *E*- and *F*-curves on the basis of the raw data (Perry and Green, 1997) while correcting for the residence time of the conductivity meter. Subsequently for every port, the Peclet number, which is a

characteristic for the plug-flow behavior of the reactor, was calculated based on the normalized variance of the residence time (Fogler, 1991).

The determination of the oxygen overall mass transfer coefficient k_{overall} of the BioScope was performed as described previously (Mashego et al., 2006; Visser et al., 2002). Water was flushed with nitrogen gas to remove all dissolved oxygen. The deoxygenated water (37 °C) was fed to the BioScope at a flow rate of 0.5, 1 and 2 ml/min, respectively. The dissolved oxygen (DO) concentration of the stream was measured at the different sampling ports using a flow cell in which a DO probe was mounted. The parameter k_{overall} was estimated from the measured DO profiles by a least sum of squares fit using MATLAB (The MathWorks Inc., Natick, MA, USA) as described by Mashego et al. (2006).

2.3. Strain and preculture conditions

Escherichia coli K12 MG1655 [λ^- , F^- , rph^{-1}] was obtained from The Netherlands Culture Collection of Bacteria (NCCB). Cells were grown to stationary phase in shake-flasks on LB medium. Culture aliquots containing 50% (v/v) glycerol were kept at -80°C until they were used as inoculum of the precultures for chemostat experiments.

Precultures were grown on minimal medium with the following composition per liter: 5.0 g (NH₄)₂SO₄, 2.0 g KH₂PO₄, 0.5 g MgSO₄ · 7H₂O, 0.5 g NaCl, 2.0 g NH₄Cl, 5.5 g glucose · 1H₂O, 0.001 g thiamine-HCl, 1 ml of trace elements solution as described by Verduyn et al. (1992) and 40 mM MOPS. The pH of the medium was adjusted to 7.0 with 1 M K₂HPO₄ before filter sterilization (pore size 0.2 μm , cellulose acetate, Whatman GmbH, Germany).

2.4. Chemostat cultivation

Aerobic glucose-limited chemostat cultures were carried out on minimal medium at a dilution rate (D) of 0.1 h⁻¹ in a 7 l laboratory bioreactor with a working volume of 4 l, controlled by weight (Applikon, Schiedam, The Netherlands). The medium composition was adapted from a previously published medium (Taymaz-Nikerel et al., 2009) to obtain a decreased chloride concentration, because too high Cl⁻ concentrations were found to interfere with the LC part of the LC-MS analysis. The composition of the low Cl⁻ minimal medium was, per liter: 1.25 g (NH₄)₂SO₄, 1.15 g KH₂PO₄, 0.5 g MgSO₄ · 7H₂O, 0.5 g NaCl, 30 g glucose · 1H₂O, 0.001 g thiamine-HCl, 2 ml of trace elements solution and 0.2 ml silicone-based antifoaming agent (BDH, Poole, UK). The composition of the trace elements solution was described in Verduyn et al. (1992). This low Cl⁻ medium allowed a steady-state biomass concentration of about 8 g DW/l. The medium was filter sterilized (pore size 0.2 μm , polyethersulfone, Sartorius, Goettingen, Germany) without pH adjustment, the final pH of the medium was around 5.

The operating conditions, measurement of off-gas (O₂/CO₂), medium feeding and steady-state conditions were as described in Taymaz-Nikerel et al. (2009). The steady state was analyzed for cell dry weight, residual glucose and total organic carbon (TOC) for biomass lysis as described in Taymaz-Nikerel et al. (2009).

2.5. Rapid sampling and metabolite quantification

Quantification of intracellular metabolites was carried out with a differential method, as described previously (Taymaz-Nikerel et al., 2009), whereby the intracellular metabolite levels were obtained from measurements in total broth and filtrate samples. Before the perturbation experiments, that is when the

culture was at steady state, broth and filtrate sampling were carried out as described in [Taymaz-Nikerel et al. \(2009\)](#). For intracellular metabolite quantification during the perturbation experiments (in the reactor as well as in the BioScope) only broth sampling was carried out because the metabolite concentrations in the filtrate did not change significantly during such experiments (not shown). Time patterns of intracellular metabolite levels during perturbation experiments were therefore obtained by subtraction of the measured amounts in the filtrate during steady-state conditions shortly before the perturbation, from the measured total broth amounts during transient conditions.

In brief, the procedure was as follows: fast sampling was carried out as described previously ([Lange et al., 2001](#)) whereby 1 ml of broth was rapidly withdrawn from the bioreactor and instantaneously quenched in tubes containing 5 ml of 60% aqueous methanol, pre-cooled at -40°C , which were immediately mixed after sampling by vortexing. For filtrate sampling, syringe filtration (pore size $0.45\ \mu\text{m}$, MILLEX-HV, Millipore, Carrigtwohill, Co. Cork, Ireland) at room temperature was employed as described in [Taymaz-Nikerel et al. \(2009\)](#). The obtained 1 ml filtrate was immediately mixed with 5 ml of 60% aqueous methanol, pre-cooled at -40°C , in order to process these samples in the same way as the broth samples. The exact amounts of sample obtained (for broth and filtrate) were quantified gravimetrically. For every steady-state condition two samples were taken and analyzed in duplicate. During perturbation experiments, one sample was taken and analyzed in duplicate for each time point.

For measurement of glucose and produced organic acids, syringe filtration (pore size $0.45\ \mu\text{m}$, MILLEX-HV, Millipore, Carrigtwohill, Co. Cork, Ireland) with cold stainless steel beads was employed ([Mashego et al., 2003](#)). For the perturbation experiments carried out directly in the chemostat, this was done simultaneously with rapid broth sampling using a second sample port. For the perturbation experiments carried out in the BioScope, each perturbation experiment was carried out twice, one for filtrate sampling and one for broth sampling. Each sample was analyzed in triplicate.

2.6. Perturbation experiments

2.6.1. In the chemostat

A moderate glucose pulse, whereby the extracellular glucose concentration was instantaneously increased from the steady-state level of $14\ \text{mg/l}$ to $500\ \text{mg/l}$ was applied. To achieve this, $20\ \text{ml}$ glucose pulse solution was directly injected into the reactor with a sterile syringe. At the same time the glucose solution was injected, the feed pump was stopped. The pump was restarted $510\ \text{s}$ after the start of the perturbation experiment.

One hour before the perturbation, the air stream for aeration of the reactor was mixed with a stream of $1.34\ \text{mol/h}$ of pure oxygen (total gassing rate $5.80\ \text{mol/h}$) which resulted in an increase of the oxygen concentration of the aeration gas to 39% (v/v). This was done to prevent the occurrence of oxygen limitation during the perturbation experiments.

2.6.2. In the BioScope

Short-term perturbation experiments were carried out using the BioScope designed for *E. coli* experiments, described above. In brief, broth was withdrawn from the chemostat at a flow rate of either 1.8 or $3.6\ \text{ml/min}$ (depending on the time scale of observation), using a peristaltic pump (ISMATEC, Glattbrugg, Switzerland). The broth was mixed with a concentrated pulse solution (0.2 or $0.4\ \text{ml/min}$ for broth flow rates of 1.8 and $3.6\ \text{ml/min}$, respectively) and pumped through the serpentine-shaped

BioScope channel. The perturbation solution contained $27.8\ \text{mM}$ glucose which resulted in the same initial bulk glucose concentration as for the perturbation carried out directly in the chemostat. The gas channel of the BioScope was continuously flushed with enriched air ($63\% \text{O}_2$) at a flow rate of $0.3\ \text{mol/h}$. For each time point one sample was taken and analyzed in duplicate.

Also for the BioScope experiments quantification of intracellular metabolites was carried out with the differential method, as described above. A sample tube (polystyrene, diameter of $17\ \text{mm}$) containing $5\ \text{ml}$ of 60% aqueous methanol (-40°C) was placed under each port of the BioScope in the cryostat (Lauda RP 1845, Lauda-Köningshofen, Germany). For each sample point $1\ \text{ml}$ of broth was withdrawn by adjusting the opening time of the valve correspondingly, i.e. $30\ \text{s}$ for a flow rate of $2\ \text{ml/min}$ and $15\ \text{s}$ for a flow rate of $4\ \text{ml/min}$. The broth was sampled directly into the cold methanol solution. The total sampling time was 300 and $105\ \text{s}$ for a flow rate of $2\ \text{ml/min}$ (all ports used) and $4\ \text{ml/min}$ (7 ports used), respectively. The sample processing procedure was the same as described in [Taymaz-Nikerel et al. \(2009\)](#).

For the measurement of the residual glucose concentration as well as organic acid production, filtrate sampling was carried out. Therefore sample tubes (polystyrene, diameter of $17\ \text{mm}$) filled with $32\ \text{g}$ stainless steel beads each were placed in a cryostat and cooled down to 0°C . From each sample port of the BioScope $3\ \text{ml}$ of broth was withdrawn into each sample tube whereby the opening time of the valve was set at $90\ \text{s}$ for a flow rate of $2\ \text{ml/min}$ and $45\ \text{s}$ for a flow rate of $4\ \text{ml/min}$. After sampling of the whole series, the content of each tube (steel beads with quenched broth of $\sim 0^{\circ}\text{C}$) was transferred to a pre-cooled syringe and directly filtered into Eppendorf tubes which were stored at -20°C until further analysis.

After each pulse experiment, the BioScope was flushed with water, ethanol and air to clean the serpentine channels and tubings. It was not needed to sterilize the BioScope before use, because the flow of broth from the bioreactor through the BioScope is one way and does not enter the reactor anymore.

2.7. Metabolite extraction procedure

Metabolites were extracted in 75% boiling ethanol ($3\ \text{min}$, 90°C) as described in [Taymaz-Nikerel et al. \(2009\)](#). Before extraction, $100\ \mu\text{l}$ of 100% U- ^{13}C -labeled cell extract was added as internal standard.

2.8. Measurement of intracellular metabolite concentrations

Metabolites of the glycolysis, TCA cycle and PPP were quantified with Isotope Dilution Mass Spectrometry (IDMS) as described by [van Dam et al. \(2002\)](#) and [Wu et al. \(2005\)](#). The concentrations of the nucleotides were also analyzed with IDMS. Further details of the applied LC-ESI-MS/MS procedure have been described elsewhere ([Seifar et al., 2009](#)).

2.9. Calculation procedures

2.9.1. Biomass-specific rates

The biomass-specific glucose consumption rate (q_s), oxygen consumption rate (q_{O_2}), carbon dioxide production rate (q_{CO_2}) and the cell lysis rate (q_{lysis}) were calculated for each chemostat cultivation from the steady-state mass balances. q_{lysis} was calculated from the difference between the measured TOC contents in the broth and in the supernatant as described in [Taymaz-Nikerel et al. \(2009\)](#). The specific growth rate, μ , in the chemostat was calculated as the sum of the dilution

rate and q_{lysis} . The reconciled rates were calculated by standard data reconciliation techniques (Verheijen, 2010).

2.9.2. Mass action ratio (MAR)

For a reaction $aA + bB \leftrightarrow cC + dD$, the corresponding mass action ratio is calculated as $(C^c D^d)/(A^a B^b)$. Hereby a , b , c and d are the stoichiometric coefficients of the reactants/products of A, B, C and D, respectively.

3. Results and discussion

3.1. BioScope characteristics

3.1.1. Pressure drop over the liquid channel of the BioScope

The observation time window of the BioScope is dependent on the total flow rate (sum of the flow rates of the perturbation agent and the culture broth) that is fed to the system and the liquid volume of the serpentine channel. An important prerequisite is not to exceed the maximum allowable liquid pressure, in order to ensure a stable flow rate and to prevent possible damage. A too high pressure drop over the liquid channel will also lead to bulging of the silicon membrane into the gas channel and result in an increase of the liquid volume which will change the residence time distribution.

The pressure drop over the liquid channel of the BioScope was measured at each sample port for flow rates between 1 and 4 ml/min. As expected, the pressure drop increases with increasing liquid flow rate and linearly increases with the channel length (not shown). At a flow rate of 2.5 ml/min and higher the measured pressure drop at some sample ports towards the end of the channel was higher than 1 bar, which we considered as the upper limit because for the peristaltic pump used a stable flow rate was not guaranteed for differential pressures above 1 bar (see Materials and methods). To avoid excessive membrane bulging and variances in the set flow rates, the pressure drop over the liquid channel was kept below 1 bar by using only a part of the liquid channel in case of flow rates exceeding 2.5 ml/min. As an example, for experiments carried out at a flow rate of 4 ml/min, sample port 8 was used as waste outlet and thus the part of the channel after port 8 was not used.

3.1.2. Residence time distribution and plug-flow characteristics

The residence time distributions for flow rates of 2 and 4 ml/min were measured fivefold and the results obtained are depicted in Fig. 2a. It was found that the residence times calculated for the first 3–4 sampling ports contained high inaccuracies (not shown). This is due to the fact that the correction made for the

contribution of the conductivity cell to the measured residence time was relatively high for these first ports, because of the small volume of the corresponding part of the channel. Therefore, we used linear regression on the RTD data obtained for the ports further downstream of the channel to determine the residence times for the first sampling ports. A total flow rate of 2 ml/min enabled to sample from all 10 ports, representing periods of exposure from 1.66 to 40.10 s. A total flow rate of 4 ml/min allowed to sample from 7 ports, representing periods of exposure from 1.06 to 8.02 s. It should be noted that the measured residence times were higher than the ones obtained from the design, e.g. at 2 ml/min the residence time for the last sample port was 40.10 s instead of the designed value of 30.2 s. The most probable reason for this is that the pressure in the liquid channel resulted in bulging of the silicone membrane into the gas channel, thus increasing the volume of the liquid channel. This shows the importance of carrying out RTD measurements instead of relying on the design parameters only.

Fig. 2b depicts the corresponding calculated Peclet numbers, which could not be calculated for the first 3 and 4 ports at flow rate 2 and 4 ml/min, respectively, for the reason outlined above, i.e. the large contribution of the volume of the conductivity cell used. It is known that when $Pe > 30$ dispersion effects can be considered negligible (Visser et al., 2002). As can be seen from Fig. 2b the calculated Peclet numbers were all close to or higher than 30 and thus proper plug-flow characteristics were obtained.

3.1.3. Oxygen transfer

The oxygen transfer characteristics of the BioScope were measured by introducing a flow of deoxygenated water into the liquid channel of the BioScope, which was subsequently oxygenated via the silicone membrane by flushing air through the opposite gas channel. The dissolved oxygen (DO) concentration of the stream was measured at the different sampling ports of the BioScope using a flow cell in which a DO probe was mounted. The obtained DO profiles for the different flow rates applied (0.5, 1 and 2 ml/min) are shown in Fig. 3a. It can be seen from this figure that the steepness of the increase of the DO vs the channel length is inversely proportional to the liquid flow rate, due to the increased liquid residence time, and thus increased time for oxygen transfer, at lower flow rates. From the obtained DO concentration profiles the overall mass transfer coefficients for oxygen (k_{overall}) for the different flow rates were estimated, the results are depicted in Fig. 3b. It can be seen from this figure that k_{overall} increases with increasing liquid flow rate, and seems to level off at higher flow rates. This is most probably the result of a decrease of the liquid boundary layer at higher flow rates. The value of k_{overall} for a flow rate of 2 ml/min was estimated to be

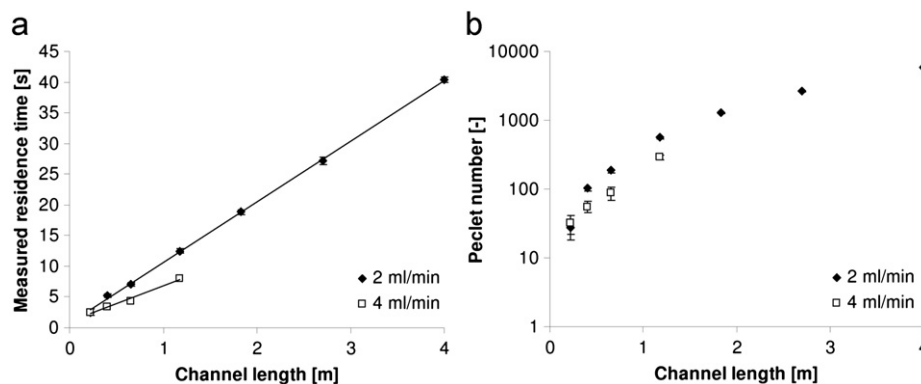


Fig. 2. BioScope characteristics. (a) Measured residence times (s) as a function of the channel length L (m) at a flow rate of 2 ml/min (diamonds) and 4 ml/min (squares). (b) Calculated Peclet number as a function of the channel length L (m) at a flow rate of 2 ml/min (diamonds) and 4 ml/min (squares).

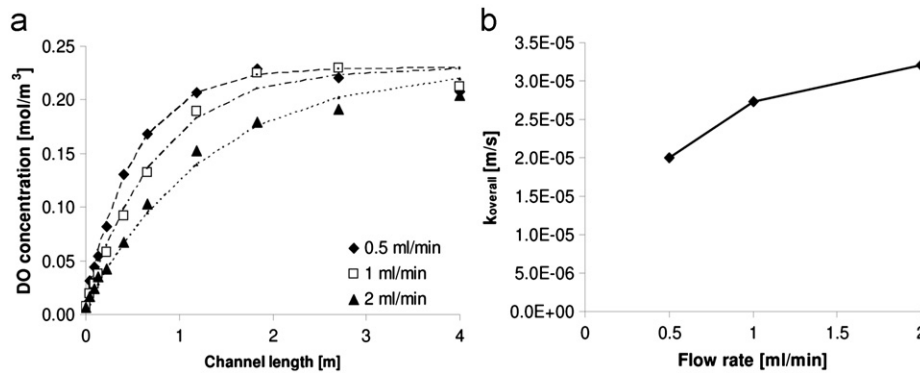


Fig. 3. (a) Measured dissolved oxygen (DO) concentration profiles with the fitted patterns that belong to the estimated $k_{overall}$ and (b) estimated $k_{overall}$ as function of different flow rates.

Table 1

Measured and reconciled data for aerobic glucose limited *E. coli* chemostat cultures at $D=0.1 \text{ h}^{-1}$, with their standard errors.

	Experiment 1		Experiment 2	
	Measured	Reconciled	Measured	Reconciled
C_x (g DW/l)	8.40 ± 0.12	8.36 ± 0.12	8.02 ± 0.12	8.02 ± 0.12
D (h^{-1})	0.101		0.105	
μ (mmol/Cmol X h)	129.5 ± 2.7	129.2 ± 2.7	136.6 ± 2.6	136.6 ± 2.6
$-q_s$ (mmol/Cmol X h)	40.78 ± 1.6	42.3 ± 1.2	44.61 ± 1.8	44.5 ± 1.3
$-q_{O_2}$ (mmol/Cmol X h)	120.3 ± 5.9	115.7 ± 4.7	125.4 ± 8.3	121.1 ± 5.8
q_{CO_2} (mmol/Cmol X h)	124.4 ± 6.1	124.6 ± 4.9	130.2 ± 8.7	130.5 ± 6.0
q_{lysis} (mmol/Cmol X h)	28.9 ± 1.6	28.9 ± 1.6	31.4 ± 1.2	31.3 ± 1.2
Carbon Recovery (%)	103.8 ± 6.1		99.7 ± 5.3	
Redox Recovery (%)	106.1 ± 5.5		101.8 ± 4.3	

$3.2 \times 10^{-5} \text{ m/s}$. This value is significantly higher than the value of $1.8 \times 10^{-5} \text{ m/s}$ estimated for BioScope II (Mashego et al., 2006), which was designed for pulse response experiments with *S. cerevisiae* and comparable to the estimated $k_{overall}$ for the first-generation BioScope ($3.0 \times 10^{-5} \text{ m/s}$) (Visser et al., 2002).

Considering the specific surface area for gas exchange of $3183 \text{ m}^2/\text{m}^3$ for a semicircular channel with a diameter of 0.8 mm, the $k_L a$ for oxygen transfer can be calculated to equal 367 h^{-1} . This is lower (albeit sufficient enough) than the $k_L a$ of the chemostat which was approx. 500 h^{-1} , as was calculated from the oxygen uptake rate and dissolved oxygen tension during steady-state chemostat cultivation of *E. coli*. From this it was concluded that the oxygen transfer capacity of the BioScope would be high enough to carry out the glucose pulse experiments while maintaining fully aerobic conditions.

3.2. Characteristics of the *E. coli* steady-state

In this study two aerobic glucose-limited steady-state chemostat cultivations on minimal medium at a dilution rate of 0.1 h^{-1} were carried out. The raw and reconciled biomass-specific rates of glucose consumption, biomass decay, biomass growth, oxygen consumption and carbon dioxide production for the two steady-state cultures are given in Table 1. The results show that the cultures were reproducible and that there were no significant differences between the reconciled and measured q -rates, indicating that during aerobic steady-state chemostat growth of *E. coli*, glucose was converted to biomass without significant amounts of byproduct formation, except cell lysis products.

Intracellular metabolite levels were obtained from measurements in total broth and culture filtrate according to Taymaz-Nikerel et al. (2009) Table 2 gives an overview of the intracellular levels of the glycolytic and TCA-cycle intermediates and nucleic

Table 2

Average intracellular levels of glycolytic and TCA-cycle intermediates, and adenine, guanine and uridine nucleotides, measured during steady-state chemostat growth ($\mu\text{mol/gDW}$).

Metabolite	Experiment 1	Experiment 2
G6P	1.22 ± 0.04	1.22 ± 0.02
F6P	0.27 ± 0.01	0.28 ± 0.01
M6P	0.40 ± 0.01	0.44 ± 0.01
Mannitol-1P	0.42 ± 0.03	0.75 ± 0.09
6PG	0.27 ± 0.01	0.22 ± 0.02
FBP	0.67 ± 0.02	0.55 ± 0.07
2PG+3PG	1.24 ± 0.04	1.38 ± 0.03
PEP	1.19 ± 0.05	1.22 ± 0.03
Pyruvate	0.43 ± 0.02	0.30 ± 0.04
Citrate ^a	1.64 ± 0.06	1.12 ± 0.02
Succinate ^a	16.55 ± 0.54	22.41 ± 0.43
Fumarate ^a	0.41 ± 0.07	0.38 ± 0.01
Malate ^a	1.35 ± 0.04	1.57 ± 0.04
ADP	1.30 ± 0.04	1.41 ± 0.05
ATP	5.30 ± 0.16	5.30 ± 0.29
GDP	0.37 ± 0.03	0.31 ± 0.03
GTP	1.42 ± 0.12	1.53 ± 0.07
UDP	0.65 ± 0.05	0.64 ± 0.05
UTP	1.00 ± 0.06	1.54 ± 0.11

^a Amount in the broth.

acids during steady-state chemostat growth for the two experiments. Most of the measured metabolite levels in the filtrate were comparable (results not shown) with previous findings (Taymaz-Nikerel et al., 2009). Also in these experiments no nucleotides were detected in the filtrate. The intracellular metabolite levels in the two independent cultures appeared very similar for most of the compounds measured, which indicates the reproducibility of our measurements/cultivations.

3.3. Perturbation experiments: comparison of reactor to BioScope

Glucose perturbation experiments were carried out directly in the chemostat (Experiment 1, time window of 40 s) and outside the chemostat by using the BioScope (Experiment 2) at two different flow rates: 2 and 4 ml/min providing observation time windows of 8 and 40 s, respectively. The dissolved oxygen concentration in the chemostat before the glucose pulse carried out in the chemostat (Experiment 1) was about 0.42 mol/m^3 (note that 100% of air saturation at 37°C and 1 bar corresponds with a dissolved oxygen concentration of 0.23 mol/m^3) because oxygen enriched air was used for aeration to prevent oxygen limitation during the pulse experiment (see materials and methods). During the glucose pulse experiment carried out in the chemostat the dissolved oxygen concentration decreased to approx. 0.35 mol/m^3 (in 40 s). For the glucose pulse carried out in the BioScope (Experiment 2), the dissolved oxygen concentration in the chemostat was 0.15 mol/m^3 because normal air was used for aeration. During the glucose pulse carried out in the BioScope the dissolved oxygen concentration never dropped below 0.14 mol/m^3 (DO measured at the last sampling port of the BioScope). These results confirm that there was no oxygen limitation during the glucose perturbation experiments both in the chemostat and in the BioScope.

Because the pH in the BioScope was not controlled, it was verified whether a significant change in the pH occurred during the glucose pulse experiment. The pH of the broth measured at the end of the serpentine channel (waste outlet) of the BioScope was 6.8, showing that the pH decreased only slightly (from pH 6.9

in the reactor to pH 6.8 at the end port of the BioScope) during the glucose pulse.

The measured dynamic patterns of the intracellular levels of the glycolytic and TCA-cycle intermediates and nucleic acids during the glucose pulse experiments carried out in the chemostat and the BioScope are shown in Figs. 4–7. Fig. 8 presents some derived quantities (mass action and relevant metabolite ratios).

It can be seen from the results shown in Figs. 4–7 that the sudden increase of the external glucose concentration from 14 mg/l to 500 mg/l led to a fast response of the intracellular metabolite concentrations. The BioScope data obtained at the two different flow rates corresponded well with each other, indicating that these pulses were well reproducible. Moreover, the dynamic metabolite patterns obtained from the BioScope pulse experiments were in most cases very similar to the patterns obtained from the pulse experiments carried out directly in the chemostat.

For the majority of the measured metabolites most of the dynamics occurs during the first 5–10 s after the pulse. This implies that to properly catch these dynamics in prokaryotes, intensive sampling at a resolution of seconds to subseconds is required, indicating once again the usefulness and necessity of the BioScope and/or similar devices. Clearly the frequency of the manual sampling carried out during the pulse experiment in the chemostat, which was approx. one sample per 5 s, was not sufficient to catch the dynamics of *E. coli*.

It can be observed from the metabolite patterns shown that after a period of about 20 s a metabolic pseudo steady state (pss) was reached. Also, the metabolic pss in *E. coli* was reached much faster than observed for yeast or filamentous fungi in similar

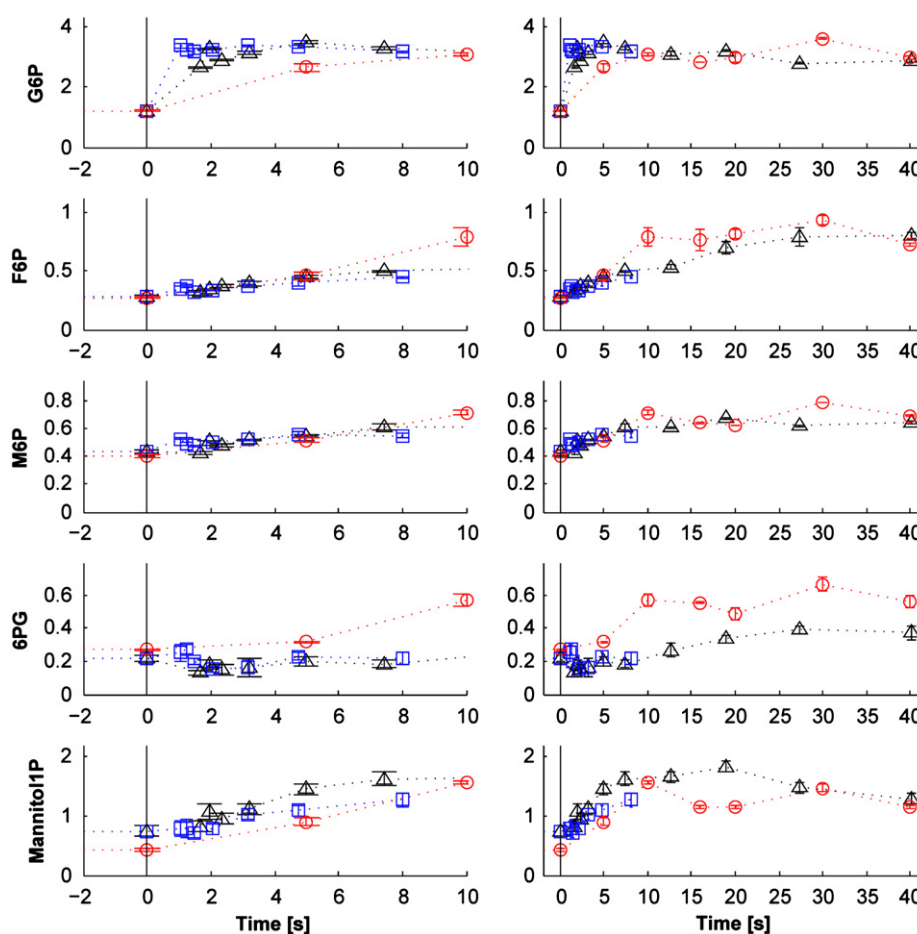


Fig. 4. Measured dynamic patterns ($\mu\text{mol/gDW}$) of glycolytic metabolites, 6PG and Mannitol1P during the glucose pulse in the reactor (Experiment 1, circles) and in the BioScope (Experiment 2, triangles: flow rate 2 ml/min, total perturbation period 40.1 s and squares: flow rate 4 ml/min, total perturbation period 8.0 s).

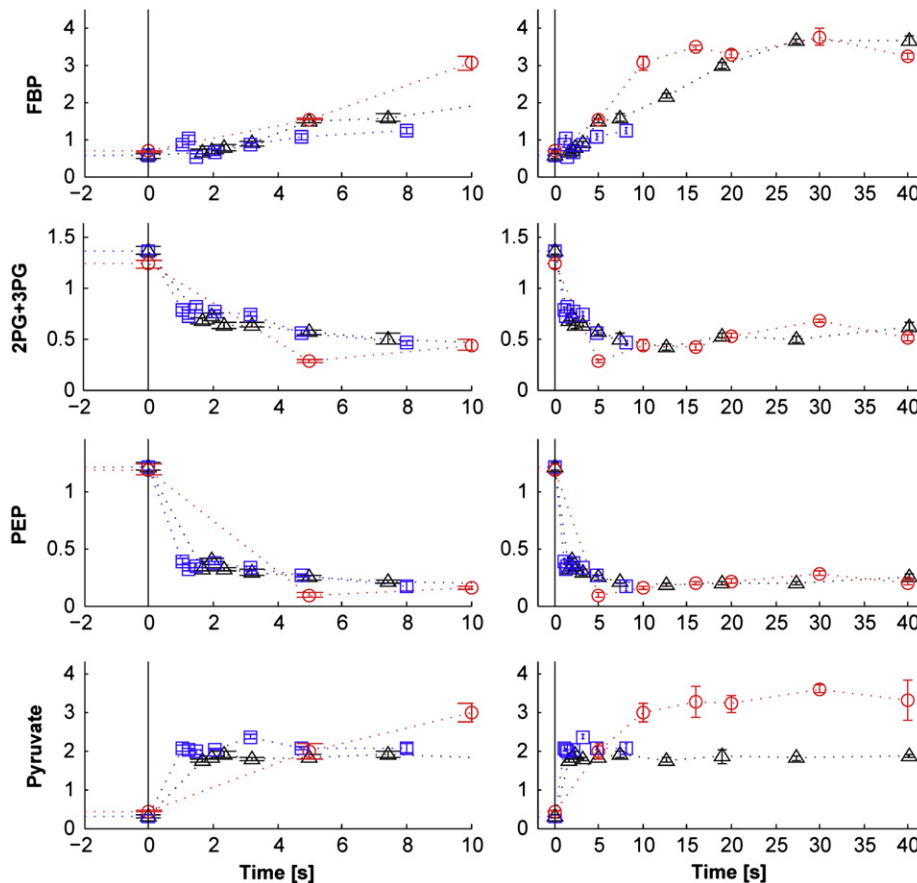


Fig. 5. Measured dynamic patterns ($\mu\text{mol/gDW}$) of lower glycolytic metabolites during the glucose pulse in the reactor (Experiment 1, circles) and in the BioScope (Experiment 2, triangles: flow rate 2 ml/min, total perturbation period 40.1 s and squares: flow rate 4 ml/min, total perturbation period 8.0 s).

glucose pulse experiments, for which this took several minutes (Mashego et al., 2006; Nasution et al., 2006; Wu et al., 2006). As can be seen from the results shown in Figs. 4–7 the measured metabolite levels during this pss appeared very similar in the BioScope and chemostat pulse experiments.

3.4. Perturbation experiments: metabolite responses

The metabolites belonging to different pathways clearly showed different dynamics (Figs. 4–7). Hereby the glycolytic intermediates showed the fastest dynamic behavior (see Figs. 4 and 5), while the changes in the levels of the TCA-cycle intermediates occurred slower (see Fig. 6). Little dynamics was observed for the adenosine, guanosine and uridine nucleotides throughout the perturbation (see Fig. 7).

The most rapidly responding metabolites were PEP, pyruvate, 2PG+3PG and G6P (see Figs. 4 and 5). The rapid decrease of PEP and corresponding increase of pyruvate clearly shows the fast response of the phosphotransferase system (PTS) through which one mol PEP is utilized for glucose translocation and phosphorylation, producing 1 mol of pyruvate. This resulted in a very large increase of the pyruvate/PEP ratio, one of the indicators of the phosphorylation state of PTS, until after about 10 s a pss was reached (see Fig. 8). The fast decrease of the PEP level corresponded with a comparable fast decrease of the level of 2PG+3PG (Fig. 5). The mass action ratio $\text{PEP}/(2\text{PG}+3\text{PG})$ also shows a fast decrease until after a few seconds a pss is reached.

The fast response of the PTS system is also reflected in the fast change of the G6P level, which increased with a factor three

within a second after the pulse. Remarkably, the F6P level increased much slower. This results in a very fast and steep decrease of the mass action ratio of PGI from 0.23, which is close to the equilibrium value of 0.32 ± 0.08 (Goldberg et al., 2004), to 0.1, followed by a slow recovery to a pss value that is close to the initial value (see Fig. 8). This suggests that the extremely fast increase of G6P induces a rapid but temporary displacement from equilibrium of PGI.

The levels of the measured hexose-phosphates G6P, F6P and M6P increased to reach a pss with values of, respectively, 3-, 3- and 2-fold their initial value. However, the dynamics during the increase of the metabolites were very different, as is reflected in the mass action ratios. Compared to the F6P/G6P ratio the M6P/F6P ratio shows a relatively slow decrease to a pss value which is about 2/3 of the initial value (Fig. 8), which might be due to an increased anabolic demand.

The fact that the intracellular levels of the nucleotides do not change significantly during the perturbation experiments shows the robustness of the energy system of *E. coli* (Fig. 7). Similar results for nucleotides were obtained in replicate perturbation experiments (data not shown).

Several authors have reported the fast metabolic response of different strains of *E. coli* K12 to glucose perturbations in an aerobic glucose-limited chemostats at a dilution rate of 0.1 h^{-1} (Buchholz et al., 2002; Chassagnole et al., 2002; Hoque et al., 2005; Schaefer et al., 1999; Schaub and Reuss, 2008). The initial glucose concentration obtained after injection of the pulse solution was either 0.3 g/l (Chassagnole et al., 2002; Schaub and Reuss, 2008) or 3 g/l (Buchholz et al., 2002; Hoque et al., 2005; Schaefer et al., 1999).

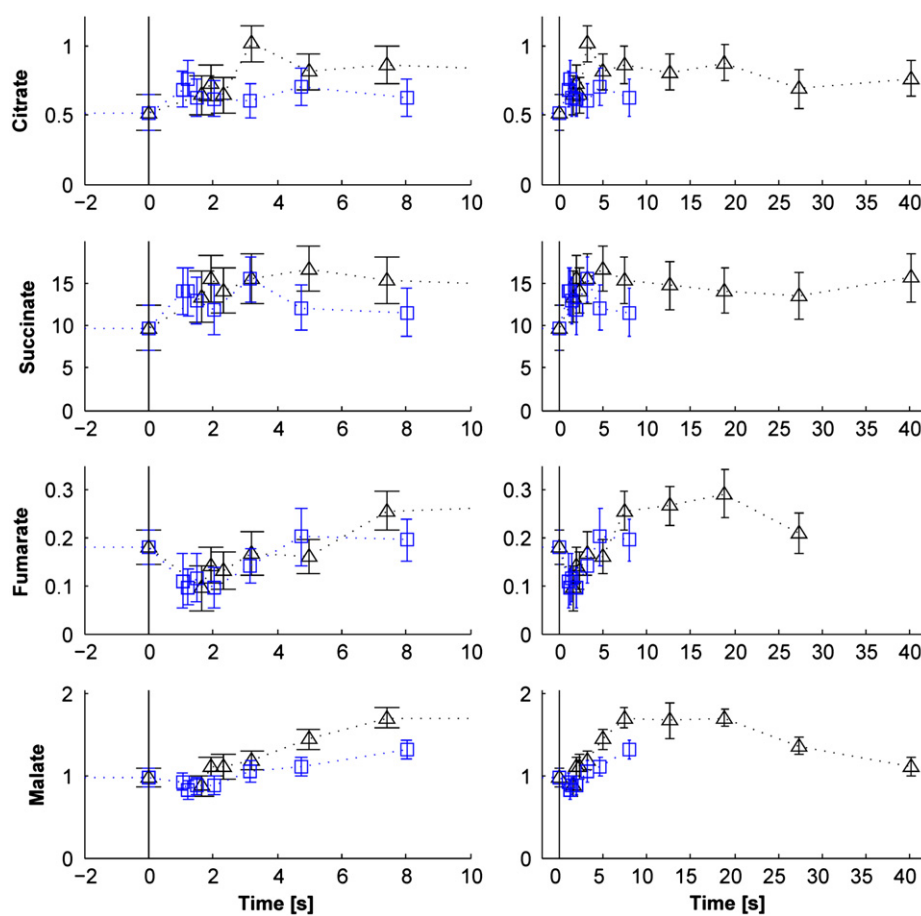


Fig. 6. Measured dynamic patterns ($\mu\text{mol/gDW}$) of TCA-cycle metabolites during the glucose pulse in the BioScope (Experiment 2, triangles: flow rate 2 ml/min, total perturbation period 40.1 s and squares: flow rate 4 ml/min, total perturbation period 8.0 s).

The sudden injection of a glucose solution into a glucose-limited chemostat results in the sudden relief of carbon-limited conditions and thus in a sharp increase of the oxygen uptake rate. However, in none of the previous studies it was reported whether special precautions were taken to prevent oxygen limitation. Furthermore no results of dissolved oxygen measurements were presented to show that oxygen non-limited conditions were maintained during the glucose perturbation.

Although the published glucose pulse experiments were carried out in a similar way, different methods for sampling, quenching, and metabolite extraction were used. Schaefer et al. (1999) and Buchholz et al. (2002) used an automated rapid sampling device whereby the sample was sprayed into a cold methanol solution (60% v/v, -50°C). After cold centrifugation, the cell pellet was extracted in cold perchloric acid. Hoque et al. (2005) also applied cold methanol quenching (60% v/v, -80°C), cold centrifugation and cold perchloric acid extraction. The advantage of the cold methanol procedure is that it allows removal of the extracellular metabolites, but has the disadvantage that part of the intracellular metabolites is lost by leakage from the cells into the cold methanol solution (Bolten et al., 2007; Taymaz-Nikerel et al., 2009). Both Chassagnole et al. (2002) and Schaub and Reuss, (2008) used total broth sampling, whereby Chassagnole et al. (2002), sampled either into liquid nitrogen (for measurement of acid labile metabolites) or in cold perchloric acid. Schaub and Reuss (2008) applied combined quenching and extraction of the broth with a helical coil heat exchanger. It should be noted that total broth extraction may lead to over-estimation of metabolite levels, depending on the amount present

in the intracellular medium. It has been shown that in *E. coli* this is indeed the case for many metabolites (Taymaz-Nikerel et al., 2009).

For several metabolites the reported response to a glucose pulse was similar to what has been measured in the present study, although the absolute levels were sometimes different, e.g. a very rapid increase (within a second) of the G6P level and corresponding decrease of PEP due to the sudden increase of glucose translocation and phosphorylation by the PTS (Buchholz et al., 2002; Schaefer et al., 1999). However, Schaefer et al. (1999) and Hoque et al. (2005) reported a decrease for both PEP and pyruvate after the glucose pulse, which is not expected when glucose uptake is mediated by the PTS. Another example to differences from our results is that both Schaefer et al. (1999) and Buchholz et al. (2002) reported a rapid decline followed by an increase of PEP. Moreover, the metabolite profiles reported by both the authors showed an oscillatory behavior, which was not observed in our experiments. Hoque et al. (2005) and Schaub and Reuss (2008) observed similar trends in the responses of 2PG+3PG and PEP after the glucose pulse, but the responses were much less fast and pronounced as observed in our experiments. Remarkably, the reported steep decline of the intracellular ATP level after subjecting the *E. coli* chemostat culture to a glucose pulse (Chassagnole et al., 2002; Hoque et al., 2005) was not observed in our experiments.

Compared to eukaryotes (*S. cerevisiae* and *P. chrysogenum*) the dynamics in *E. coli* are much faster (about factor 7) but similar profiles of metabolites can be observed (Mashego et al., 2007; Nasution et al., 2006). For pyruvate, a different profile in yeast was

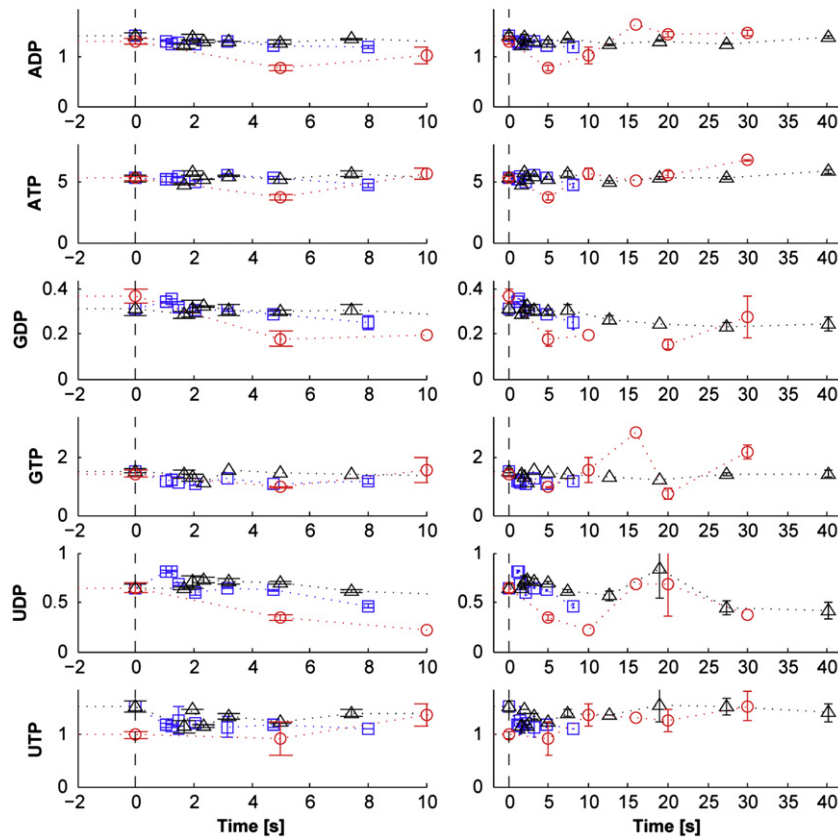


Fig. 7. Measured dynamic patterns ($\mu\text{mol/gDW}$) of nucleotides during the glucose pulse in the reactor (Experiment 1, circles) and in the BioScope (Experiment 2, triangles: flow rate 2 ml/min, total perturbation period 40.1 s and squares: flow rate 4 ml/min, total perturbation period 8.0 s).

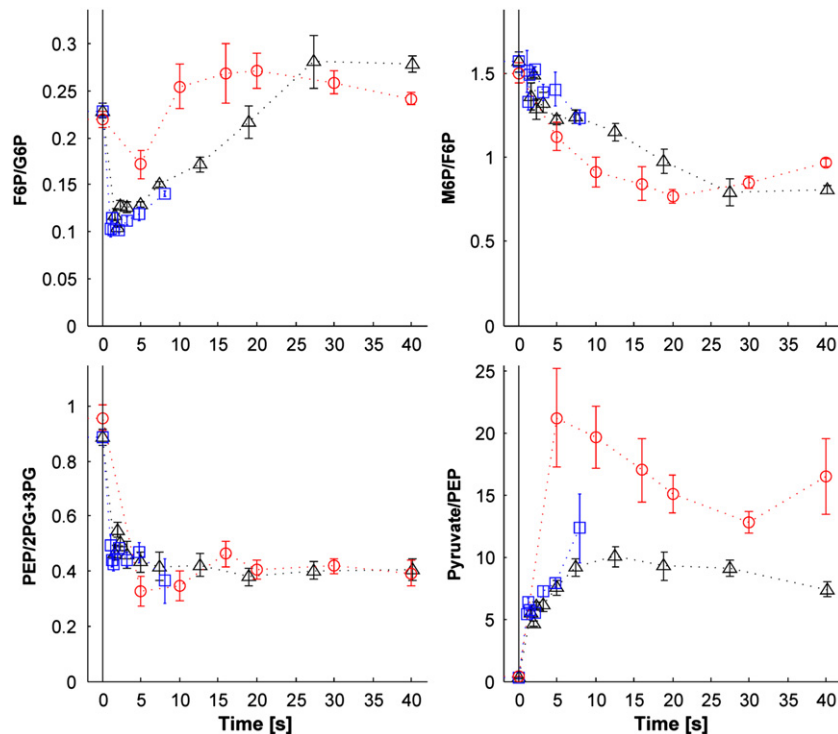


Fig. 8. Calculated mass action ratios (MAR) for phosphoglucose isomerase (PGI), mannose-6P isomerase (PMI), combined enolase (ENO), phosphoglucomutase (PGM) and PYR/PEP ratio during the glucose pulse in the chemostat (Experiment 1, circles) and in the BioScope (Experiment 2, triangles: flow rate 2 ml/min, total perturbation period 40.1 s and squares: flow rate 4 ml/min, total perturbation period 8.0 s).

observed due to the fact that yeast does not have the PTS. Another difference we observed is that the intracellular nucleotide levels do not change much during a glucose pulse in *E. coli*, whereas a sharp decrease in the ATP level was observed in eukaryotes (Mashego et al., 2007; Nasution et al., 2006).

4. Conclusions

Metabolic responses of *E. coli* to glucose pulses were efficiently determined within a short time period (40 s) in an adapted BioScope system. Metabolite responses were shown to differ with respect to relative concentration changes and dynamic behavior. The good agreement between the dynamic patterns of several glycolytic, TCA-cycle intermediates and nucleotides in *E. coli* after a glucose pulse carried out directly in the chemostat and in the BioScope demonstrates that the BioScope is a promising device for studying *in vivo* kinetics. Additionally, the BioScope system has the advantage that it allows withdrawal of sufficient sample volume for extensive metabolite analysis. An important aspect which has often been neglected is to maintain aerobic conditions during rapid perturbation experiments. It was shown that oxygen transfer in the BioScope is sufficient to achieve this.

Kinetic metabolic models appear necessary in order to fully exploit the information on the complex *in vivo* regulation of metabolic networks. The analysis of metabolome data after a glucose pulse can be complemented by investigations aiming at performing different perturbation experiments to obtain richer kinetic data that would increase our understanding quantitatively.

Acknowledgments

The authors wish to thank Arno van den Berg, Dirk Geerts and Rob Kerste for the construction of the BioScope, Johan Knoll for the TOC measurements, and Reza Seifar and Zhen Zeng for the LC-MS/MS analysis of the metabolites. This research was performed in the framework of an IWT-SBO project MEMORE (040125) financially supported by the Institute for the Promotion of Innovation through Science and Technology in Flanders (IWT Vlaanderen). This project was carried out within the research program of the Kluuyver Centre for Genomics of Industrial Fermentation which is part of the Netherlands Genomics Initiative/Netherlands Organization for Scientific Research.

References

Bolten, C.J., Kiefer, P., Letisse, F., Portais, J.C., Wittmann, C., 2007. Sampling for metabolome analysis of microorganisms. *Analytical Chemistry* 79 (10), 3843–3849.

Buchholz, A., Hurlbeaus, J., Wandrey, C., Takors, R., 2002. Metabolomics: quantification of intracellular metabolite dynamics. *Biomolecular Engineering* 19 (1), 5–15.

Buziol, S., Bashir, I., Baumeister, A., Claaßen, W., Noisommit-Rizzi, N., Mailinger, W., Reuss, M., 2002. New bioreactor-coupled rapid stopped-flow sampling technique for measurements of metabolite dynamics on a subsecond time scale. *Biotechnology and Bioengineering* 80, 632–636.

Chassagnole, C., Noisommit-Rizzi, N., Schmid, J.W., Mauch, K., Reuss, M., 2002. Dynamic modeling of the central carbon metabolism of *Escherichia coli*. *Biotechnology and Bioengineering* 79 (1), 53–73.

Chou, I.C., Voit, E.O., 2009. Recent developments in parameter estimation and structure identification of biochemical and genomic systems. *Mathematical Biosciences* 219 (2), 57–83.

de Koning, W., van Dam, K., 1992. A method for the determination of changes of glycolytic metabolites in yeast on a subsecond time scale using extraction at neutral pH. *Analytical Biochemistry* 204 (1), 118–123.

Fogler, S., 1991. *Elements of Chemical Reaction Engineering*. Prentice-Hall International Editions, New Jersey.

Goldberg, R.N., Tewari, Y.B., Bhat, T.N., 2004. Thermodynamics of enzyme-catalyzed reactions—a database for quantitative biochemistry. *Bioinformatics* 20 (16), 2874–2877.

Hoque, M.A., Ushiyama, H., Tomita, M., Shimizu, K., 2005. Dynamic responses of the intracellular metabolite concentrations of the wild type and *pykA* mutant *Escherichia coli* against pulse addition of glucose or NH₃ under those limiting continuous cultures. *Biochemical Engineering Journal* 26 (1), 38–49.

Kresnowati, M.T., Suarez-Mendez, C.M., van Winden, W.A., van Gulik, W.M., Heijnen, J.J., 2008. Quantitative physiological study of the fast dynamics in the intracellular pH of *Saccharomyces cerevisiae* in response to glucose and ethanol pulses. *Metabolic Engineering* 10 (1), 39–54.

Krömer, J.O., Wittmann, C., Schroder, H., Heinze, E., 2006. Metabolic pathway analysis for rational design of L-methionine production by *Escherichia coli* and *Corynebacterium glutamicum*. *Metabolic Engineering* 8 (4), 353–369.

Lange, H.C., Eman, M., van Zuijlen, G., Visser, D., van Dam, J.C., Frank, J., de Mattos, M.J., Heijnen, J.J., 2001. Improved rapid sampling for *in vivo* kinetics of intracellular metabolites in *Saccharomyces cerevisiae*. *Biotechnology and Bioengineering* 75 (4), 406–415.

Mashego, M.R., van Gulik, W.M., Heijnen, J.J., 2007. Metabolome dynamic responses of *Saccharomyces cerevisiae* on simultaneous rapid perturbations in external electron acceptor and electron donor. *FEMS Yeast Research* 7 (1), 48–66.

Mashego, M.R., van Gulik, W.M., Vinke, J.L., Heijnen, J.J., 2003. Critical evaluation of sampling techniques for residual glucose determination in carbon-limited chemostat cultures of *Saccharomyces cerevisiae*. *Biotechnology and Bioengineering* 83 (4), 395–399.

Mashego, M.R., van Gulik, W.M., Vinke, J.L., Visser, D., Heijnen, J.J., 2006. *In vivo* kinetics with rapid perturbation experiments in *Saccharomyces cerevisiae* using a second-generation BioScope. *Metabolic Engineering* 8 (4), 370–383.

Nasution, U., van Gulik, W.M., Proell, A., van Winden, W.A., Heijnen, J.J., 2006. Generating short-term kinetic responses of primary metabolism of *Penicillium chrysogenum* through glucose perturbation in the BioScope minireactor. *Metabolic Engineering* 8 (5), 395–405.

Nikerel, I.E., van Winden, W.A., Verheijen, P.J., Heijnen, J.J., 2009. Model reduction and a priori kinetic parameter identifiability analysis using metabolome time series for metabolic reaction networks with linlog kinetics. *Metabolic Engineering* 11 (1), 20–30.

Perry, R., Green, D., 1997. *Perry's Chemical Engineers' Handbook*. McGraw-Hill, New York.

Schaefer, U., Boos, W., Takors, R., Weuster-Botz, D., 1999. Automated sampling device for monitoring intracellular metabolite dynamics. *Analytical Biochemistry* 270 (1), 88–96.

Schaub, J., Reuss, M., 2008. *In vivo* dynamics of glycolysis in *Escherichia coli* shows need for growth-rate dependent metabolome analysis. *Biotechnology Progress* 24 (6), 1402–1407.

Seifar, R.M., Ras, C., van Dam, J.C., van Gulik, W.M., Heijnen, J.J., van Winden, W.A., 2009. Simultaneous quantification of free nucleotides in complex biological samples using ion pair reversed phase liquid chromatography isotope dilution tandem mass spectrometry. *Analytical Biochemistry* 388 (2), 213–219.

Stephanopoulos, G., 1999. Metabolic fluxes and metabolic engineering. *Metabolic Engineering* 1, 1–11.

Taymaz-Nikerel, H., de Mey, M., Ras, C., ten Pierick, A., Seifar, R.M., van Dam, J.C., Heijnen, J.J., van Gulik, W.M., 2009. Development and application of a differential method for reliable metabolome analysis in *Escherichia coli*. *Analytical Biochemistry* 386 (1), 9–19.

Teusink, B., Passarge, J., Reijenga, C.A., Esgalhadó, E., van der Weijden, C.C., Schepper, M., Walsh, M.C., Bakker, B.M., van Dam, K., Westerhoff, H.V., et al., 2000. Can yeast glycolysis be understood in terms of *in vitro* kinetics of the constituent enzymes? Testing biochemistry. *European Journal of Biochemistry* 267 (17), 5313–5329.

Theobald, U., Mailinger, W., Reuss, M., Rizzi, M., 1993. *In vivo* analysis of glucose-induced fast changes in yeast adenine nucleotide pool applying a rapid sampling technique. *Analytical Biochemistry* 214, 31–37.

van Dam, J.C., Eman, M.R., Frank, J., Lange, H.C., van Dedem, G.W.K., Heijnen, S.J., 2002. Analysis of glycolytic intermediates in *Saccharomyces cerevisiae* using anion exchange chromatography and electrospray ionization with tandem mass spectrometric detection. *Analitica Chimica Acta* 460 (2), 209–218.

Verduyn, C., Postma, E., Scheffers, W.A., van Dijken, J.P., 1992. Effect of benzoic acid on metabolic fluxes in yeasts: a continuous-culture study on the regulation of respiration and alcoholic fermentation. *Yeast* 8 (7), 501–517.

Verheijen, P.J.T., 2010. Data reconciliation and error detection. In: Smolke, C.D. (Ed.), *The Metabolic Pathway Engineering Handbook. Fundamentals*. CRC Press, Boca Raton, FL.

Visser, D., van Zuylen, G.A., van Dam, J.C., Oudshoorn, A., Eman, M.R., Ras, C., van Gulik, W.M., Frank, J., van Dedem, G.W., Heijnen, J.J., 2002. Rapid sampling for analysis of *in vivo* kinetics using the BioScope: a system for continuous-pulse experiments. *Biotechnology and Bioengineering* 79 (6), 674–681.

Wiechert, W., 2002. Modeling and simulation: tools for metabolic engineering. *Journal of Biotechnology* 94 (1), 37–63.

Wu, L., Mashego, M.R., van Dam, J.C., Proell, A.M., Vinke, J.L., Ras, C., van Winden, W.A., van Gulik, W.M., Heijnen, J.J., 2005. Quantitative analysis of the microbial metabolome by isotope dilution mass spectrometry using uniformly ¹³C-labeled cell extracts as internal standards. *Analytical Biochemistry* 336, 164–171.

Wu, L., van Dam, J., Schipper, D., Kresnowati, M.T., Proell, A.M., Ras, C., van Winden, W.A., van Gulik, W.M., Heijnen, J.J., 2006. Short-term metabolome dynamics and carbon, electron, and ATP balances in chemostat-grown *Saccharomyces cerevisiae* CEN.PK 113-7D following a glucose pulse. *Applied and Environmental Microbiology* 72 (5), 3566–3577.